Solid State Phase Equilibria in the Er-Ni-P and Er-Ni-As Systems at 800 °C

Mariya Zelinska[a,b], Olga Zhak[a], Stepan Oryshchyn[a], Tetiana Polianska[a], and Jean-Yves Pivan[b]

[a] Department of Analytical Chemistry, Ivan Franko National University of Lviv, Kyryla & Mefodija Str. 6, 79005 Lviv, Ukraine
[b] Laboratoire de Chimie du Solide et Inorganique Moléculaire, UMR CNRS 6511, Université de Rennes 1 - ENSCR, Institut de Chimie, Campus de Beaulieu, Avenue du Général Leclerc, 35042 Rennes Cedex, France

Reprint requests to Dr. S. Oryshchyn. E-mail: ndch@franko.lviv.ua

Z. Naturforsch. **2007**, *62b,* 1143 – 1152; received March 14, 2007

Solid-state phase equilibria in the ternary systems Er-Ni-P and Er-Ni-As have been determined at 800 °C (region 0 – 67 at. % P or 0 – 50 at. % As) using X-ray diffraction, scanning electron microscopy and electron probe microanalysis. Eight ternary phosphides and six ternary arsenides have been synthesized, including several phases reported previously. The hexagonal structure of the new compound $Er_6Ni_{20}P_{13}$, as determined from single-crystal X-ray data, exhibits a new structure type closely related to the $Ho_6Ni_{20}P_{13}$ structure. Two other new phosphides, $Er_{16}Ni_{36}P_{22}$ ($Tb_{16}Ni_{36}P_{22}$-type) and $Er_{20}Ni_{42}P_{30}$ ($Sm_{20}Ni_{41.6}P_{30}$-type), have also been obtained at 800 °C. In the Er-Ni-As system, a new arsenide $Er_{20}Ni_{42}As_{30}$ ($Sm_{20}Ni_{41.6}P_{30}$-type) has been found in addition to known ternary phases. From X-ray powder data, the structures of the ternary arsenides $ErNi_4As_2$ ($ZrFe_4Si_2$-type) and $Er_2Ni_{12}As_7$ ($Zr_2Fe_{12}P_7$-type) have been refined by Rietveld methods. In the single crystal investigations, two other new phases $Er_{12}Ni_{30}P_{21}$ [derived $(La, Ce)_{12}Rh_{30}P_{21}$-type] and $Er_{13}Ni_{25}As_{19}$ ($Tm_{13}Ni_{25}As_{19}$-type) have been prepared by high-temperature annealing (1500 °C).

Key words: Rare Earth Compounds, Phosphide, Arsenide, Phase Diagram, Crystal Structure

Introduction

The ternary *Ln*-Ni-P systems, where *Ln* represents a heavy rare earth metal, have been investigated systematically for *Ln* = Y, Gd, Tb, Ho, and Yb [1 – 5], and the corresponding isothermal sections of the solid-state phase diagrams have been constructed for the temperature of 800 °C, in the concentration region of 0 – 67 at. % P. In general, these systems showed about six to eight ternary phosphides, the crystal structures of which have been determined [6, 7]. On the contrary, the ternary systems *Ln*-Ni-As have not been studied widely, except for Y-Ni-As [1] and Ho-Ni-As [8], for which the isothermal sections of the phase diagrams have been constructed at 800 °C (concentration range 0 – 70 at. % As). Five ternary arsenides have been observed in each system, and their crystal structures have been determined [1, 7, 8]. In addition, numerous ternary compounds *Ln*-Ni-{P, As} have been synthesized and structurally characterized [6, 7]. To give an example, in the Er-Ni-P system, six ternary phosphides have been reported: $ErNi_4P_2$ [9], $Er_{25}Ni_{49}P_{33}$ [10], $Er_2Ni_{12}P_7$ [11], $Er_7Ni_{19}P_{13}$ [12], ErNiP [13], and $ErNi_2P_2$ [14], while in the Er-Ni-As system five ternary arsenides have been identified: $ErNi_4As_2$ [15], $Er_2Ni_{12}As_7$ [16], $Er_7Ni_{19}As_{13}$ [12], ErNiAs [17], and Er_2NiAs_2 [18]. The crystallographic data of these phases are summarized in Table 1.

In order to continue our systematic investigations on the *Ln*-Ni-{P, As} systems, we focus in this paper on the interaction of erbium with nickel and phosphorus or arsenic. Crystallographic data and structure refinements of new ternary phases as well as the construction of the isothermal section of the solid state phase diagrams Er-Ni-P and Er-Ni-As for the temperature of 800 °C have been established.

Experimental Determination of the Er-Ni-P and Er-Ni-As Phase Diagrams

Experimental details

Several different synthetic procedures were used for the sample preparation depending on the P or As content. Starting materials were ingots of erbium (stated purity 99.99 wt. %), and powders of nickel, red phosphorus or gray arsenic (all with a minimum purity of 99.98 wt. %). In a first

Table 1. Crystallographic data of the ternary Er-Ni-P and Er-Ni-As compounds.

[a] Phases synthesized at high temperature.

Compound	Space group	Structure type	Lattice parameters (nm)		Ref.
			a	*c*	
$ErNi_4P_2$	$P4_2/mnm$	$ZrFe_4Si_2$	0.7094	0.3605	[9]
			0.70770(7)	0.35985(4)	this work
$Er_{16}Ni_{36}P_{22}$	$P\bar{6}m2$	$Tb_{16}Ni_{36}P_{22}$	1.7943(5)	0.37706(8)	this work
$Er_{25}Ni_{49}P_{33}$	$P\bar{6}m2$	$Sm_{25}Ni_{49}P_{33}$	2.1756	0.3790	[10]
			2.1794(3)	0.37751(7)	this work
$Er_{20}Ni_{42}P_{30}$	$P\bar{6}_3/m$	$Sm_{20}Ni_{41.6}P_{30}$	2.0177(2)	0.37720(7)	this work
$Er_2Ni_{12}P_7$	$P\bar{6}$	$Zr_2Ni_{12}P_7$	0.9037	0.3667	[11]
			0.90442(4)	0.36660(2)	this work
$Er_7Ni_{19}P_{13}$	$P\bar{6}$	$Zr_6Ni_{20}P_{13}$	1.2648	0.3721	[12]
$Er_6Ni_{20}P_{13}$	$P6_3/m$	own	1.26351(3)	0.37326(1)	this work
ErNiP	$P6_3/mmc$	$Tb_{1-x}NiP$	0.3905	1.5086	[13]
$Er_{0.91}NiP$			0.38916(1)	1.50335(7)	this work
$ErNi_2P_2$	$I4/mmm$	$CeAl_2Ga_2$	0.3830	0.9303	[14]
			0.3851(3)	0.9307(9)	this work
$Er_{12}Ni_{30}P_{21}$	$P6_3/m$	own	1.63900(3)	0.37573(1)	this work[a]
$ErNi_4As_2$	$P4_2/mnm$	$ZrFe_4Si_2$	0.7215	0.3758	[15]
			0.72162(2)	0.37573(1)	this work
$Er_2Ni_{12}As_7$	$P\bar{6}$	$Zr_2Fe_{12}P_7$	0.9344	0.3795	[16]
			0.93505(3)	0.37981(1)	this work
$Er_7Ni_{19}As_{13}$	$P\bar{6}$	$Zr_6Ni_{20}P_{13}$	1.3061	0.3839	[12]
$Er_6Ni_{20}As_{13}$			1.30798(4)	0.38308(2)	this work
$Er_{20}Ni_{42}As_{30}$	$P6_3/m$	$Sm_{20}Ni_{41.6}P_{30}$	2.0935(3)	0.39009(6)	this work
$Er_{13}Ni_{25}As_{19}$	$P\bar{6}$	derived $Tm_{13}Ni_{25}As_{19}$	1.6286(2)	0.39002(4)	this work[a]
ErNiAs	$P\bar{6}m2$	YbPtP	0.4044	0.3771	[17]
			0.40444(8)	0.37657(7)	this work
Er_2NiAs_2	$P6_3/mmc$	Zr_2NiAs_2	0.4083	1.3724	[18]
			0.4081(2)	1.3753(8)	this work

step, freshly filed chips of erbium were mixed with stoichiometric amounts of the powders and pressed into pellets (1 g each) at a pressure of about 5 MPa. Samples containing less than 25 at. % P (or As) were treated by arc melting of the pellets under a Ti/Zr-gettered argon atmosphere. The samples containing 25 – 33 at. % P (As) were pre-reacted in evacuated silica tubes by gradually heating them to 800 °C (heating rate of 200 °C per day) and keeping the temperature for 3 – 5 days, followed by slow cooling to r. t. The samples were then melted in an arc furnace, turned over and re-melted several times. Finally, to reach thermodynamic equilibrium, the so-obtained samples (less than 33 at. % P or As) were again sealed into evacuated silica ampoules, which were heated at 800 °C for 800 – 1000 h, and then quenched in cold water. Finally, samples containing more than 33 at. % P (As) were just sintered at 800 °C.

In order to obtain single crystals of selected ternary compounds, a special synthesis mode was used. The pre-reacted pellets (800 °C) were placed in sealed molybdenum crucibles, heated at 1500 °C for 2 d in a high-temperature graphite furnace and then slowly cooled to r. t.

The samples were characterized by X-ray diffraction. Phase analysis of the binary and ternary compounds, as well as the intensity data collection for Rietveld structure refinement of the ternary phases, were performed using the powder diffractometers DRON-3M or HZG 4a (in both cases: CuK_α radiation with $\lambda = 1.54185$ Å, $\theta - 2\theta$ scan, $2\theta \leq 100°$, step: 0.05° in 2θ, exposure time: 15 – 20 s per step), and INEL CPS 120 (monochromatized CuK_{α_1} radiation with $\lambda = 1.540562$ Å, 2θ range: 10 – 100°, exposure time 20 min per step). All calculations were done using the CSD software package [25].

For the single-crystal structure determination, the intensity data were collected at ambient temperature with the help of a Nonius Kappa CCD diffractometer with MoK_α radiation ($\lambda = 0.71073$ Å) using the program COLLECT [26]. Data reduction and reflection indexing were performed with the program DENZO of the Kappa CCD software package [26], while structure refinement and Fourier syntheses were carried out with the program CSD [25].

Further details of the crystal structure investigations may be obtained from Fachinformationszentrum Karlsruhe, 76344 Eggenstein-Leopoldshafen, Germany (fax: +49-7247-808-666; e-mail: crysdata@fiz-karlsruhe.de, http://www.fiz-informationsdienste.de/en/DB/icsd/depot_anforderung.html) on quoting the deposition number CSD-418034.

Phase analyses by scanning electron microscopy and electron probe microanalyses by X-ray energy-dispersive spec-

troscopy (EDS) were performed using a JEOL JSM-6400 microscope. The compositions were correlated with the diffraction data in order to identify the phases present in each sample and to establish the ternary phase diagram. In the same way, some single crystals were analyzed.

The binary compounds

Fundamental information concerning the binary systems Er-Ni, Er-P or Er-As and Ni-P or Ni-As was taken from literature data [6, 7, 19]. The Er-Ni phase diagram has been widely investigated in the whole concentration range, and the formation of eleven binary compounds has been observed [7, 19]. The intermetallic compounds ErNi (FeB-type) and $ErNi_5$ ($CaCu_5$-type) melt congruently at 1100 and 1380 °C, respectively, while Er_3Ni (Fe_3C-type structure), Er_3Ni_2 (own type), $ErNi_2$ ($MgCu_2$-type), $ErNi_3$ ($NbBe_3$-type), and Er_2Ni_{17} (Th_2Ni_{17}-type) are the products of peritectic reactions at 845, 800, 1255, 1320, and 1315 °C, respectively. The binary Er_2Ni_7 decomposes peritectoidally at 1275 °C into $ErNi_3$ and $ErNi_4$. This phase exhibits two structural modifications: β-Er_2Ni_7 (rhombohedral symmetry, Er_2Co_7-type) [20] and α-Er_2Ni_7 (hexagonal symmetry, Ce_2Ni_7-type) [21], but the exact polymorphic transition temperature is unknown as yet. For the concentration region close to ~80 at. % Ni, three binary compounds, $ErNi_4$ ($PuNi_4$-type), Er_4Ni_{17} and Er_5Ni_{22}, have been reported, but only the crystal structure of $ErNi_4$ has been determined. The temperatures of the peritectic decomposition of these compounds are very close to each other (~1380 °C) [19].

For the Er-P system, the existence of two phosphides ErP (NaCl-type) and ErP_5 (NdP_5-type) has been mentioned [6, 7], but the phase diagram has not been determined. In contrast, the Er-As phase diagram has been studied in the whole concentration range and the only established compound is the monoarsenide ErAs with a NaCl structure [7, 19].

The Ni-P phase diagram has been constructed in the concentration range 0 – 40 at. % P [19]. The binary compound Ni_5P_2 melts congruently at 1175 °C and undergoes a polymorphic transition at 1025 °C. For α-Ni_5P_2, the real composition is in fact Ni_8P_3, and the structure is of a new type [22], while the structure of β-Ni_5P_2 has not been determined in the initial studies [7]. However, in a further investigation [23], the crystal structure of α-Ni_5P_2 was determined from single-crystal X-ray data, and a new structure type with trigonal symmetry was proposed. However, the results of precise quantitative phase analyses of the binary Ni-P samples in the concentration range 28 – 32 at. % P did not confirm the formation of the Ni_8P_3 phase at 800 °C [23]. The other binary phosphides Ni_3P (Fe_3P-type), $Ni_{12}P_5$ (own type), Ni_2P (Fe_2P-type), Ni_5P_4 (own type), and NiP_2 (PdP_2-type), are formed peritectically and exist over extended temperature ranges [19]. The compounds $Ni_{\sim 1.22}P$ (unknown structure), NiP (own structure type), and NiP_3 ($CoAs_3$-type) have been isolated only at high temperatures [7]. Finally, the phosphide NiP_2 with the pyrite-type structure was synthesized under high pressure (6.5 GPa) at temperatures between 1100 °C and 1400 °C [7].

The Ni-As phase diagram has been studied in the concentration range up to 70 at. % As, and the formation of four binary arsenides has been observed: $Ni_{11}As_8$, Ni_5As_2, NiAs, and $NiAs_2$ [7, 19]. Most of these phases have crystal structures of their own types. The arsenides NiAs and Ni_5As_2 melt congruently at 970 °C and near 1000 °C, and exhibit homogeneity ranges of 50 – 61.3 and 28.09 – 28.74 at. % As, respectively [19]. According to the literature [24], NiAs presents a modulated structure at r. t. Finally, $NiAs_2$ undergoes a polymorphic transition at 593 °C. α-$NiAs_2$ crystallizes with its own type, while β-$NiAs_2$ has an orthorhombic structure of the marcasite-type at normal pressure, and a cubic one (pyrite-type) at high pressure and high temperature (6 GPa and 1400 °C) [7].

The Er-Ni-P phase diagram

On the basis of the binary compounds mentioned above, the isothermal section of the Er-Ni-P phase diagram has been constructed (800 °C, up to 67 at. % P). Solid-state phase equilibria in the Er-Ni-P system have been established using X-ray diffraction and scanning electron microscopy of 39 samples (Fig. 1). It is worth mentioning that all binary compounds on the phase diagram have been confirmed at the reaction temperature. No extended solid solutions based on the binary and ternary compounds have been observed.

The existence of the previously reported ternary compounds $ErNi_4P_2$, $Er_{25}Ni_{49}P_{33}$, $Er_2Ni_{12}P_7$, ErNiP, and $ErNi_2P_2$ has been confirmed. Refinement of the unit cell parameters are compared with those from literature data in

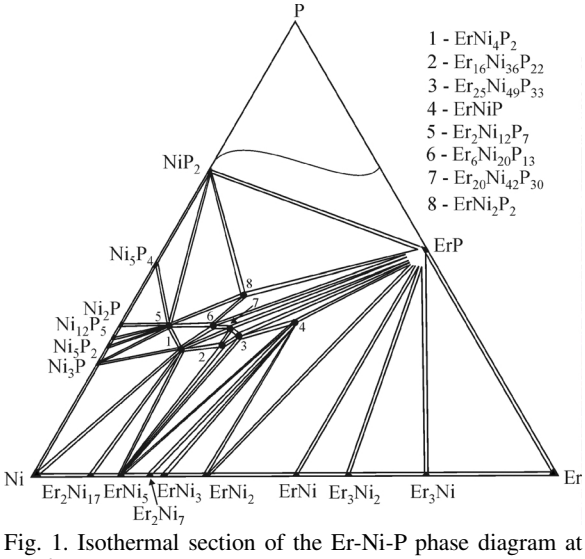

Fig. 1. Isothermal section of the Er-Ni-P phase diagram at 800 °C (0 – 67 at. % P).

Table 1. In agreement with our recent structure refinements of the ternary phosphides $ErNi_4P_2$, $Er_{25}Ni_{49}P_{33}$, and ErNiP [27], it can be concluded that the latter compound in reality has a composition $Er_{0.96}NiP$ (or $Er_{1-x}NiP$ with $x = 0.04$), since the Wyckoff position 2*a* is not fully occupied.

The new X-ray single crystal structure determination of $Er_6Ni_{20}P_{13}$ has invalidated the formula $Er_7Ni_{19}P_{13}$ given previously in literature [12]. The refinement led to a new structure type, which is nevertheless closely related to the $Ho_6Ni_{20}P_{13}$ type (*vide infra*).

Two new ternary phosphides, $Er_{16}Ni_{36}P_{22}$ and $Er_{20}Ni_{42}P_{30}$, have been isolated at 800 °C, and their lattice parameters suggest isotypism with the $Tb_{16}Ni_{36}P_{22}$ [28] and $Sm_{20}Ni_{41.6}P_{30}$ structures [29], respectively (Table 1).

Finally, during attempts to obtain single crystals of the latter phosphides, another ternary compound, $Er_{12}Ni_{30}P_{21}$, could be isolated for the first time, but at a higher temperature, *i. e.*, at 1500 °C. The structure is closely related to the $(La,Ce)_{12}Rh_{30}P_{21}$-type [30]. The description of the crystal structure together with the magnetic properties of the new compound $Er_{12}Ni_{30}P_{21}$ will be the subject of a future paper.

The Er-Ni-As phase diagram

The isothermal section of the Er-Ni-As phase diagram at 800 °C has been constructed from X-ray phase analysis of 25 samples in the concentration range 0 – 50 at. % As (Fig. 2). The existence of numerous binary phases in the Er-Ni, Er-As and Ni-As systems, which border the phase diagram at 800 °C, has been confirmed. No extended solid solutions based on the binary and ternary phases have been observed.

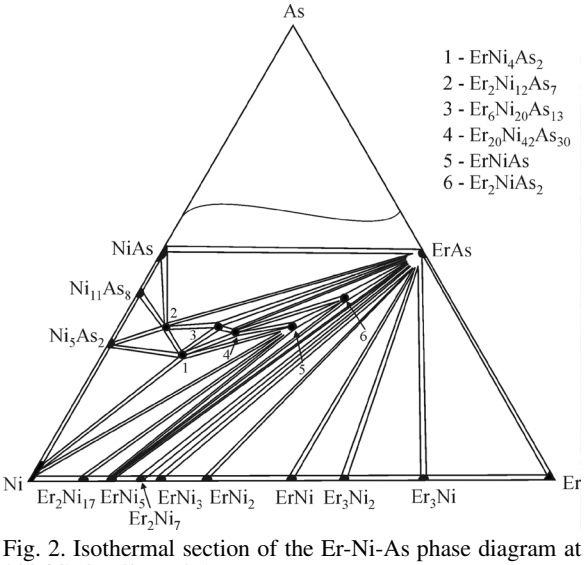

Fig. 2. Isothermal section of the Er-Ni-As phase diagram at 800 °C (0 – 50 at. % As).

Table 2. Crystal structure data and structure refinement of $Er_6Ni_{20}P_{13}$.

Empirical formula	$Er_6Ni_{20}P_{13}$
Formula weight, g mole^{-1}	2580.42
Crystal size, mm^3	$0.13 \times 0.04 \times 0.025$
Crystal system	hexagonal
Space group; Z	$P6_3/m$; 1
a, nm	1.26351(3)
c, nm	0.37326(1)
V, nm^3	0.52(1)
$D_{calc.}$, g cm^{-3}	8.28(1)
Linear absorption coeff., mm^{-1}	43.6
hkl range	$-22 < h < 22$; $-22 < k < 22$; $-5 < l < 6$
$(\sin\theta/\lambda)_{max}$, nm^{-1}	0.0903
Collected reflections	12162
Unique reflections	1187
R_{int}	0.049
Variable parameters	50
$R(F)/wR(F^2)$ (all reflections)	0.051 / 0.055
Scale factor	1.004(2)
GOF (F^2)	1.030
$\Delta\rho_{fin}$ (max/min), e Å^{-3}	3.85/−2.55

The existence of the previously reported ternary arsenides $ErNi_4As_2$, $Er_2Ni_{12}As_7$, $Er_6Ni_{20}As_{13}$, ErNiAs, and Er_2NiAs_2 has also been confirmed. A new ternary compound, with approximate composition $Er_{20}Ni_{42}As_{30}$, has been synthesized for the first time. Refinement of the hexagonal unit cell parameters suggested isotypism with the $Sm_{20}Ni_{41.6}P_{30}$ structure (Table 1). However, our attempts to obtain single crystals or a pure X-ray powder pattern in order to confirm this hypothesis were unsuccessful.

The crystallographic data for the ternary compounds in the Er-Ni-As phase diagram at 800 °C are summarized in Table 1. A new ternary compound $Er_{13}Ni_{25}As_{19}$ could be prepared at high temperatures (about 1300 – 1500 °C), the crystal structure of which belongs to the $Tm_{13}Ni_{25}As_{19}$-type [31]. Structural details of this structure will be the subject of a future publication.

Crystal structure of $Er_6Ni_{20}P_{13}$

Madar *et al.* [12] previously obtained a series $Ln_7Ni_{19}X_{13}$, where *Ln* = Y, La, Ce, Pr, Nd, Sm, Gd, Tb, Dy, Ho, Er, Tm, and *X* = P, As. According to X-ray powder analyses, this family shows isotypism with $Zr_6Ni_{20}P_{13}$ [32]. However, samples supposed to have the ideal composition $Ln_6Ni_{20}X_{13}$ always contained admixtures of $Ln_2Ni_{12}X_7$. Therefore, an additional stucture determination seemed necessary to validate these first results.

The phosphide $Er_6Ni_{20}P_{13}$ was synthesized by reaction of ErP, NiP and Ni at 800 °C in an evacuated quartz ampoule. Single crystals of $Er_6Ni_{20}P_{13}$ could be isolated from a crushed sample. Details of the intensity data collection and refinement are summarized in Table 2. From the inten-

Table 3. Positional and anisotropic displacement parameters for $Er_6Ni_{20}P_{13}$.

Atom	Wyckoff position	occ, %	*x/a*	*y/b*	*z/c*	B_{eq} ($\times 10^2$ nm^2)	B_{11}	B_{22}	B_{33}	B_{12} ($B_{13} = B_{23} = 0$).
Er1	6*h*	100	0.47075(5)	0.28170(5)	3/4	0.63(1)	0.66(2)	0.65(2)	0.60(2)	0.34(1)
Ni1	2*d*	100	2/3	1/3	1/4	0.68(4)	0.65(5)	0.66(2)	0.74(9)	0.33(2)
Ni2	6*h*	100	0.3206(2)	0.0744(2)	1/4	0.78(4)	0.77(5)	0.76(5)	0.83(6)	0.41(4)
Ni3	6*h*	100	0.4364(2)	0.0204(2)	3/4	0.74(4)	0.78(5)	0.76(5)	0.73(5)	0.41(4)
Ni4	6*h*	40.0(9)	0.0751(4)	0.1576(5)	1/4	1.20(11)	0.41(11)	0.89(13)	2.1(2)	0.17(10)
Ni5	6*h*	49.6(9)	0.1983(3)	0.1053(3)	3/4	0.91(8)	1.03(11)	0.72(10)	1.06(11)	0.51(9)
Ni6	6*h*	11.4(9)	0.0408(13)	0.1002(13)	1/4	0.64(15)	–	–	–	–
P1	2*a*	33(3)	0	0	1/4	1.2(2)	–	–	–	–
P2	6*h*	100	0.5247(3)	0.1392(3)	1/4	0.54(7)	0.60(8)	0.38(8)	0.52(9)	0.17(7)
P3	6*h*	100	0.2818(3)	0.2319(3)	1/4	0.73(8)	0.80(9)	0.88(10)	0.66(9)	0.53(8)

Table 4. Interatomic distances (nm) for the $Er_6Ni_{20}P_{13}$ structure with esd.'s given in units of the last significant digit in parentheses.

Er:	2 P3	0.2842(3)	Ni4:	1 P3	0.2291(7)	P1:	6 Ni6	0.2168(9)
	2 P2	0.2885(3)		4 Ni4	0.2542(5)		3 Ni5	0.2171(4)
	2 P2	0.2901(3)		2 P1	0.2542(4)		6 Ni4	0.2542(4)
	2 Ni1	0.29020(5)		2 P3	0.2558(5)		6 Ni5	0.2863(3)
	2 Ni2	0.2996(2)		1 Ni2	0.2633(6)	P2:	1 Ni1	0.2199(4)
	2 Ni3	0.3022(2)		2 Ni5	0.2715(5)		1 Ni2	0.2281(4)
	1 Ni5	0.3024(4)		2 Ni5	0.2736(5)		1 Ni3	0.2302(4)
	1 Ni3	0.3105(2)		2 Ni2	0.2819(4)		2 Ni3	0.2303(2)
	1 Ni3	0.3107(2)		1 Er	0.3468(6)		2 Er	0.2885(3)
	1 Ni2	0.3112(2)	Ni5:	1 P3	0.2204(6)		2 Er	0.2901(3)
	2 Er	0.37326(1)		2 P3	0.2338(4)	P3:	1 Ni5	0.2204(6)
	2 Er	0.38492(9)		1 Ni2	0.2474(5)		1 Ni3	0.2273(5)
Ni1:	3 P2	0.2199(4)		2 Ni2	0.2575(3)		1 Ni2	0.2276(5)
	6 Er	0.29020(5)		2 Ni4	0.2715(5)		1 Ni4	0.2291(7)
Ni2:	1 P3	0.2276(5)		2 Ni4	0.2736(5)		2 Ni2	0.2333(3)
	1 P2	0.2281(4)		4 Ni5	0.2863(5)		2 Ni5	0.2338(4)
	2 P3	0.2333(3)		1 Er	0.3024(4)		2 Ni4	0.2558(5)
	1 Ni5	0.2474(5)	Ni6:	2 Ni4	0.2349(11)		2 Er	0.2842(3)
	2 Ni5	0.2575(3)		1 Ni4	0.241(2)			
	1 Ni4	0.2633(6)		2 Ni4	0.2458(12)			
	2 Ni3	0.2661(2)		1 Ni4	0.252(2)			
	2 Ni4	0.2819(4)		2 Ni5	0.2594(12)			
	1 Ni6	0.2.86(6)		1 P3	0.264(2)			
	2 Er	0.2996(2)		2 Ni5	0.2706(13)			
	1 Er	0.3112(2)		1 Ni5	0.283(2)			
Ni3:	1 P3	0.2273(5)		1 Ni2	0.286(2)			
	1 P2	0.2302(4)		2 P3	0.2914(13)			
	2 P2	0.2303(2)		1 Ni5	0.293(2)			
	2 Ni2	0.2661(2)						
	2 Ni3	0.2677(2)						
	2 Er	0.3022(2)						
	1 Er	0.3105(2)						
	1 Er	0.3107(2)						

sity data set, the Laue symmetry 6/*m* was determined, and in accord with the systematic extinctions 00*l* ($l = 2n$) the centrosymmetric space group $P6_3/m$ was subsequently confirmed.

The structure was solved by Direct Methods (MULTAN) which resulted in the positions of all erbium and part of the nickel and phosphorus atoms. Next, the remaining nickel positions 6*h* and phosphorus positions 6*h* and 2*a* were localized step by step from successive Fourier syntheses. Refinement of the occupancy factors revealed the partial occupancy of the sites 6*h* by three nickel atoms located around the 6_3 axis: Ni4 (40.0(9) %), Ni5 (49.6(9) %) and Ni6 (11.4(9) %). In the same way, the atom P1 in the 2*a* site was found to have an occupancy of only 33(3) %. Anisotropic displacement parameters for all positions occupied by more than 50 % were included in the last refinement cycles. The final results are summarized in Tables 3 and 4. The crystal structure determination led to the composition $Er_6Ni_{20.06(1)}P_{12.67(1)}$, close to $Er_6Ni_{20}P_{13}$. Energy-dispersive analysis of several crystals by scanning electron microscopy confirmed the presence of

Table 6. Positional and anisotropic displacement parameters for $ErNi_4As_2$.

Atom	Wyckoff position	*x/a*	*y/b*	*z/c*	B_{eq} ($\times 10^2$ nm^2)	B_{11}	B_{22}	B_{33}	B_{12} ($B_{13} = B_{23} = 0$)
Er	2*b*	0	0	1/2	0.95(6)	0.96(8)	0.96(8)	0.93(14)	0.24(15)
Ni	8*i*	0.3482(5)	0.0926(4)	0	1.23(11)	1.7(2)	0.5(2)	1.6(2)	−0.38(13)
As	4*g*	0.2160(3)	0.7840(3)	0	0.96(8)	1.04(11)	0.96(8)	0.8(2)	0.33(14)

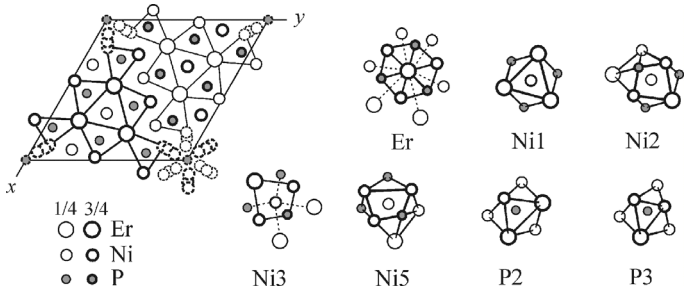

Fig. 3. Projection of the $Er_6Ni_{20}P_{13}$ structure onto the *ab* plane and coordination polyhedra of the atoms. The basic structural fragments $[Er_3Ni_{10}P_6]$ at z = 1/4 and z = 3/4 are emphasized.

Table 5. Crystal data and structure refinement for $ErNi_4As_2$ and $Er_2Ni_{12}As_7$.

Empirical formula	$ErNi_4As_2$	$Er_2Ni_{12}As_7$
Crystal system, space group	tetragonal	hexagonal
	$P4_2/mnm$ (No. 136)	$P\bar{6}$ (No. 174)
a, nm	0.72162(2)	0.93505(3)
c, nm	0.37573(1)	0.37981(1)
Cell volume, *V*, nm^3	0.19566(3)	0.28758(3)
Number of atoms in cell	14	21
Calculated density, g cm^{-3}	9.37(1)	9.03(1)
Absorption coefficient (mm^{-1})	77.5	69.7
Radiation; λ, Å	CuK_α; 1.54185	
Diffractometer	HZG-4a	DRON-3M
Mode of refinement	Full profile	
Number of atomic sites	3	9
Number of variable parameters	16	23
Range of 2θ, deg	10 – 140	
$(\sin\theta/\lambda)_{max}$, Å^{-1}	0.608	
Scale factor	0.981(3)	0.842(1)
Texture axis; parameter	[001]; 1.12(2)	–
Final *R* values R_I/ R_P	0.083/0.156	0.069/0.166
Software	CSD97	

Table 7. Positional and isotropic displacement parameters for $Er_2Ni_{12}As_7$.

Atom	Wyckoff position	*x/a*	*y/b*	*z/c*	B_{iso} ($\times 10^2$ nm^2)
Er1	1*c*	2/3	1/3	1/2	0.66(10)
Er2	1*f*	1/3	2/3	0	0.72(10)
Ni1	3*j*	0.4361(13)	0.0503(13)	0	1.1(3)
Ni2	3*j*	0.1476(10)	0.2710(6)	0	0.80(13)
Ni3	3*k*	0.3796(11)	0.4248(11)	1/2	1.1(2)
Ni4	3*k*	0.2125(6)	0.0977(10)	1/2	1.13(13)
As1	1*a*	0	0	0	0.61(12)
As2	3*j*	0.4099(8)	0.2906(10)	0	1.07(15)
As3	3*k*	0.1150(9)	0.4078(7)	1/2	0.67(13)

Table 8. No. of compounds in the ternary systems *Ln*-Ni-{P, As} (*Ln* = heavy rare earth metal); for references see text.

Ln	P		As	
Y	8	phase diagram known	5	phase diagram known
Gd	8	phase diagram known	6	–
Tb	8	phase diagram known	7	–
Dy	5	–	7	–
Ho	6	phase diagram known	5	phase diagram known
Er	9	phase diagram known; this work	7	phase diagram known; this work
Tm	5	–	5	–
Yb	7	phase diagram known	3	–
Lu	3	–	3	–

erbium, nickel and phosphorus as the only components in atomic percentages of Er : Ni : P = 16.1 : 51.0 : 32.9 (with estimated standard deviations of 2 %).

The interatomic distances in the $Er_6Ni_{20}P_{13}$ structure are listed in Table 4. A projection of the $Er_6Ni_{20}P_{13}$ structure onto the *ab* plane and the coordination polyhedra of the atoms are shown in Fig. 3.

Crystal structure of $ErNi_4As_2$

The crystal structure of the ternary arsenide $ErNi_4As_2$ could not be determined in all its details [15]. From the tetragonal symmetry and the unit cell parameters, the isotypy with the $ZrFe_4Si_2$-type was proposed. During the phase diagram construction, we obtained very pure samples of this arsenide, which enabled us to refine the $ErNi_4As_2$ structure from X-ray powder data.

The powder diffraction pattern has been successfully indexed with the tetragonal unit cell parameters listed in Table 5. The positional and anisotropic displacement parameters were refined by full-profile Rietveld methods (Table 6). The results confirm that $ErNi_4As_2$ crystallizes in the $ZrFe_4Si_2$-type, space group $P4_2/mnm$. Experimental and calculated profiles are shown in Fig. 4.

Crystal structure of $Er_2Ni_{12}As_7$

The occurrence of pure samples of the phase $Er_2Ni_{12}As_7$ enabled us to refine the crystal structure from X-ray pow-

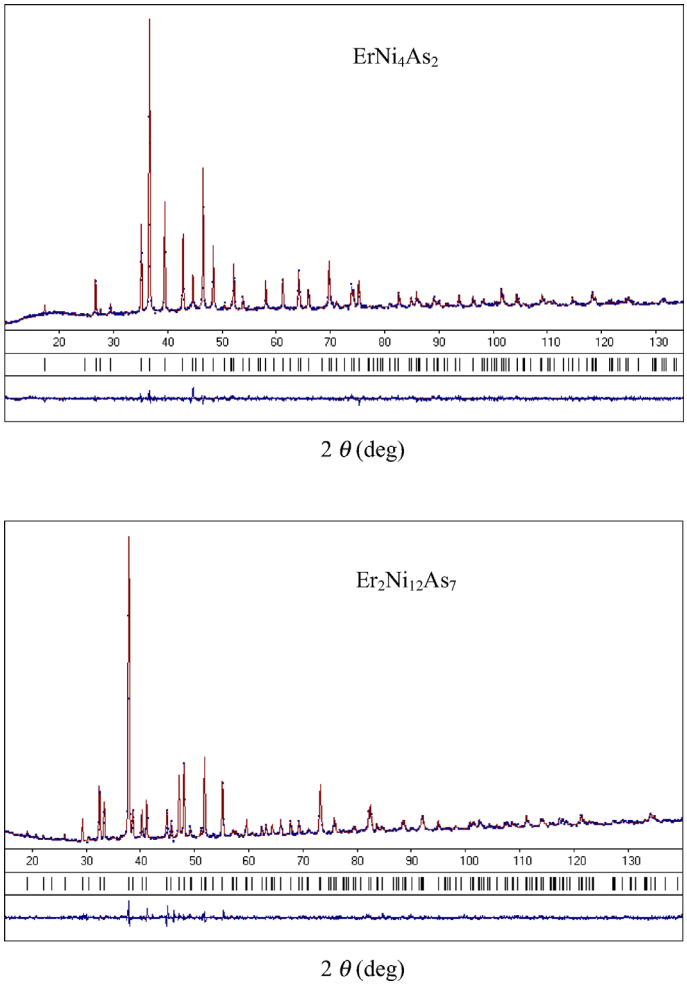

Fig. 4. Calculated (lines) and experimental (dotted lines) powder diffraction patterns of the arsenides $ErNi_4As_2$ and $Er_2Ni_{12}As_7$.

der data. The conditions of data collection and refinement are summarized in Table 5, while the positional and isotropic displacement parameters are listed in Table 7. Experimental and calculated profiles of $Er_2Ni_{12}As_7$ are presented in Fig. 4. One can conclude that $Er_2Ni_{12}As_7$ is indeed isostructural with $Zr_2Fe_{12}P_7$.

Discussion

Neither solid solutions based on the binary phosphides or arsenides under consideration nor homogeneity ranges for the ternary phases were observed in the solid-state phase equilibria of the Er-Ni-P and Er-Ni-As systems at 800 °C. On the other hand, the Er-Ni-P system presents eight ternary phosphides instead of six arsenides for the Er-Ni-As system. A comparison of the main features of these phase diagrams with those of {Y, Tb, Ho}-Ni-P and Y-Ni-As previously reported in the literature confirms the main role played by the rare earth monophosphides and monoarsenides in these phase diagrams, since more ternary phases are in thermodynamic equilibrium with these binaries (Figs. 1 and 2). Moreover, the interactions in the ternary systems depend strongly on the nature of the rare earth metal, because the number of ternary phases is not always the same (see Table 8). Indeed, with Lu, only three ternary phosphides exist, while with Y, Gd and Tb eight phases have been found.

Another general rule for all systems *Ln*-Ni-P and *Ln*-Ni-As concerns the fact that the domain of the ternary phosphides and arsenides with the heavy rare earth metals represents 10 – 40 at. % *Ln* and 25 – 40 at. % P (As). Two additional phases, $Er_{12}Ni_{30}P_{21}$ and $Er_{13}Ni_{25}As_{19}$, have been syn-

Table 9. Structure types found for the ternary compounds *Ln*-Ni-P (*Ln* = heavy rare earth metal).

Ln	Y	Gd	Tb	Dy	Ho	Er	Tm	Yb	Lu	
Structure type										Ref.
$ZrFe_4Si_2$	+	+	+	+	+	+	+	+	+	[9]
$Tb_{16}Ni_{36}P_{22}$		+	+	+		+				[28, this work]
$Sm_{25}Ni_{49}P_{33}$		+	+	+	+	+				[10]
$Sm_{20}Ni_{41.6}P_{30}$	+					+				[34, this work]
$Tb_{15}Ni_{28}P_{21}$	+		+							[1, 29]
$Zr_2Fe_{12}P_7$	+	+	+	+	+	+	+	+	+	[11]
$Ho_5Ni_{19}P_{12}$					+					[35, 36]
$Yb_5Ni_{19}P_{12}$								+		[37]
$Ho_{20}Ni_{66}P_{43}$					+					[35, 38]
$Zr_6Ni_{20}P_{13}$	+	+	+	+	+	+	+	+		[12, 39]
$Ho_6Ni_{20}P_{13}$					+					[35, 40]
$Er_6Ni_{20}P_{13}$						+				this work
$Er_{12}Ni_{30}P_{21}$						+				this work
$Y_6Ni_{15}P_{10}$	+									[41]
$Nd_3Ni_7P_5$		+	+							[42]
$Tb_{1-x}NiP$	+	+	+	+	+	+	+	+	+	[13, 14]
$CeAl_2Ga_2$	+	+	+	+	+	+	+	+		[14, 43]

Table 10. Structure types found for the ternary compounds *Ln*-Ni-As (*Ln* = heavy rare earth metal).

Ln	Y	Gd	Tb	Dy	Ho	Er	Tm	Yb	Lu	
Structure type										Ref.
$ZrFe_4Si_2$	+	+	+	+	+	+	+	+	+	[15, 44]
$Zr_2Fe_{12}P_7$	+	+	+	+	+	+	+	+	+	[16, 45]
$Zr_6Ni_{20}P_{13}$	+	+	+	+	+	+	+			[12]
$Y_6Ni_{20}As_{13}$	+									[1]
$Tb_6Ni_{15}As_{10}$	+	+	+	+						[46]
$(La,Ce)_{12}Rh_{30}P_{21}$	+		+	+						[1, 47]
$Tm_{13}Ni_{25}As_{19}$						+	+	+	+	[31, this work]
$Sm_{20}Ni_{41.6}P_{30}$	+	+	+	+		+				[17, this work]
YbPtP	+	+	+	+	+	+	+			[1, 17, 48]
Zr_2NiAs_2			+	+	+	+	+	+		[17, 18, 48]

thesized, but only at higher temperatures (above 1000 °C).

From a crystallographic point of view, all the ternary phases in general are stoichiometric with a regular distribution of the atoms on the crystallographic positions, with the exception of the compounds having the $Tb_{1-x}NiP$-type where a defect in the rare earth occupancy is observed.

In the Er-Ni-P and Er-Ni-As systems, numerous ternary phases are formed with a metalloid content of 33 at. % representing a metal/metalloid ratio of up to 2 : 1. Moreover, the ternaries $Er_2Ni_{12}P_7$ ($Er_2Ni_{12}As_7$), $Er_6Ni_{20}P_{13}$ ($Er_6Ni_{20}As_{13}$) and $Er_{20}Ni_{42}P_{30}$ ($Er_{20}Ni_{42}As_{30}$), together with the binary phosphide Ni_2P, belong to a homologous series of hexagonal two-layer structures, with the general formula $R_{n(n-1)}M_{(n+1)(n+2)}X_{n(n+1)+1}$ [6, 33]. The combination of the trigonal prisms of the *R* and M atoms (rare earths and nickel) centered by the P or As atoms are the main structural units in these compounds.

A summary of the ternary phases in the systems *Ln*-Ni-P and *Ln*-Ni-As is listed in Tables 9 and 10 featuring numerous isostructural compounds. The more common structures correspond to the types $ZrFe_4Si_2$, $Zr_2Fe_{12}P_7$, $Zr_6Ni_{20}P_{13}$ (or to the related $Ho_6Ni_{20}P_{13}$-type), $Sm_{20}Ni_{41.6}P_{30}$, and $CeAl_2Ga_2$. The present work confirms the existence of the ternary phosphide $Er_6Ni_{20}P_{13}$ instead of $Er_7Ni_{19}P_{13}$, as was previously reported by Madar *et al.* [12]. The structure of $Er_6Ni_{20}P_{13}$ is of a new type but closely related to the $Ho_6Ni_{20}P_{13}$-type (hexagonal symmetry, centrosymmetric space group $P6_3/m$) [36, 41]. The latter is derived from the $Zr_6Ni_{20}P_{13}$-type (non-centrosymmetric space group $P\bar{6}$) [12]. The main difference between the two structures $Er_6Ni_{20}P_{13}$ and $Ho_6Ni_{20}P_{13}$ results from the splitting of the Ni atoms around the sixfold axis and the occupancy factor of the phosphorus atom on this axis. Indeed, for $Er_6Ni_{20}P_{13}$ the structure refinement was done with three constrained split positions 6*h* (40 % Ni4, 49 % Ni5 and 11 % Ni6), while for $Ho_6Ni_{20}P_{13}$ two split positions (50 % Ni4 and 50 % Ni5) were refined. These atoms are represented by dotted lines in the projection of the crystal structure of $Er_6Ni_{20}P_{13}$ in Fig. 3. As commonly observed in pnictide chemistry for hexagonal crystal structures with space group $P6_3/m$ and a metal/metalloid ratio equal or close to 2, the splitting of the Ni atom position induces also a disorder in the occupancy of the position 2*a* of the P atoms on the sixfold axis. This position is only half-occupied by one P atom, since the heights ($z = 1/4$ and $3/4$) are very close to each other, as it is the case for $Ho_6Ni_{20}P_{13}$. For $Er_6Ni_{20}P_{13}$, this occupancy factor is less and corresponds to 33 %, as based on the structure refinement (Table 3).

The coordination polyhedra of the different atoms in the two structures are very similar. We have not taken into account the coordination polyhedra of the atoms occupying less than 50 % in the $Er_6Ni_{20}P_{13}$ structure (Fig. 3). The P2 and P3 atoms occupy trigonal prisms formed by the metal atoms, with three additional atoms outside the lateral faces. This is the most widespread type of coordination geometry for phosphorus atoms in intermetallic compounds [7].

Interatomic distances (Table 4) in the $Er_6Ni_{20}P_{13}$ structure (not taking into account the distances between atoms with partially occupied positions)

are close to the sum of the metallic radii of Er (0.1757 nm) and/or Ni (0.1246 nm) and the covalent radius of P (0.110 nm) [49]. The shortest distances (d = 0.2199 nm) are observed between the atoms Ni1 and P2, which correspond to a contraction of *ca.* 6.5 %.

The same comments on the coordination polyhedra and the interatomic distances hold true for the crystal structures of $ErNi_4As_2$ and $Er_2Ni_{12}As_7$. Interatomic distances in these compounds are in good agreement with the sum of the metallic radii of Er and/or Ni and the covalent radius of As (0.118 nm). The shortest distances in the two structures are the Ni-As distances, *i. e.*, 0.2377 and 0.2197 nm for $ErNi_4As_2$ and $Er_2Ni_{12}As_7$, respectively. In the latter, the contraction is nearly 12 % with respect to the sum of the respective radii. This fact can be taken to be indicative of partial covalent Ni-As bonding.

Conclusion

The investigation of the solid state phase equilibria in the ternary systems Er-Ni-P and Er-Ni-As at 800 °C led to the construction of the phase diagrams in the concentration ranges 0 – 67 at. % P and 0 – 50 at. % As. Eight ternary phosphides and six arsenides have been identified in these systems at 800 °C. Two additional phases, $Er_{16}Ni_{36}P_{22}$ and $Er_{13}Ni_{25}As_{19}$, were synthesized at higher temperatures (1300 – 1500 °C). Finally, three new phosphides ($Er_{16}Ni_{36}P_{22}$, $Er_{20}Ni_{42}P_{31}$, $Er_{12}Ni_{30}P_{21}$) and two new arsenides ($Er_{20}Ni_{42}As_{31}$, $Er_{13}Ni_{25}As_{19}$) were obtained for the first time and their unit cell parameters have been refined. Moreover, the X-ray crystal structures of $Er_6Ni_{20}P_{13}$ (single crystals), $ErNi_4As_2$ and $Er_2Ni_{12}As_7$ (powder data) have been determined and allowed to establish the structural relationships.

[1] S. Stoyko, S. Oryshchyn, *IX Intern. Conf. on Crystal Chemistry of Intermetallic Compounds*, Lviv (Ukraine), **2005**, p. 58.

[2] Yu. B. Kuz'ma, S. I. Chykhrij, *Zh. Neorg. Khim*. **1999**, *44*, 135 – 137.

[3] S. I. Chykhrij, Yu. B. Kuz'ma, *Zh. Neorg. Khim*. **1990**, *35*, 3203 – 3207.

[4] Yu. A. Mozharivskyj, Yu. B. Kuz'ma, *Dopov. Ukr. Akad. Nauk*. **1996**, *9*, 136 – 138.

[5] Yu. Kuz'ma, S. I. Chykhrij, S. L. Budnyk, *J. Alloys Comp*. **2000**, *298*, 190 – 194.

[6] Yu. B. Kuz'ma, S. I. Chykhrij, in *Handbook of the Physics and Chemistry of Rare Earths*, Vol. 23 (Eds.: K. A. Gschneider, Jr., L. Eyring), Elsevier, Amsterdam, **1996**, chapter 156, pp. 285 – 434 (Phosphides).

[7] P. Villars, L. D. Calvert, *Pearson's Handbook of Crystallographic Data for Intermetallic Phases*, Vol. 1 – 2, ASM International, Materials Park, Ohio, **1997**, p. 2886.

[8] Yu. A. Mozharivskyj, Yu. B. Kuz'ma, *Inorg. Mater*. **1998**, *34*, 254 – 256.

[9] S. I. Chykhrij, S. V. Oryshchyn, Yu. B. Kuz'ma, *Dopov. Akad. Nauk. Ukr. RSR, Ser. A* **1986**, *7*, 79 – 81.

[10] S. I. Chykhrij, V. S. Babizhetskyy, Yu. B. Kus'ma, *Z. Anorg. Allg. Chem*. **2001**, *627*, 1319 – 1324.

[11] W. Jeitschko, B. Jaberg, *Z. Anorg. Allg. Chem*. **1980**, *467*, 95 – 104.

[12] R. Madar, P. Chaudouet, E. Dhahri, J. P. Senateur, R. Fruchart, B. Lambert, *J. Solid State Chem*. **1985**, *56*, 335 – 342.

[13] S. I. Chykhrij, S. V. Oryshchyn, Yu. B. Kuz'ma, *Zh. Neorg. Khim*. **1987**, *32*, 2375 – 2379.

[14] R. Marchand, W. Jeitschko, *J. Solid State Chem*. **1978**, *24*, 351 – 357.

[15] W. Jeitschko, L. J. Terbüchte, E. J. Reinbold, P. G. Pollmeier, T. Vomhof, *J. Less-Common Met*. **1990**, *161*, 125 – 134.

[16] W. Jeitschko, B. Jaberg, *J. Less-Common Met*. **1981**, *79*, 311 – 314.

[17] V. Babizhetskyy, C. Le Sénéchal, J. Bauer, S. Députier, R. Guérin, *J. Alloys Comp*. **1999**, *287*, 174 – 180.

[18] E. H. El Ghadrahoui, J.-Y. Pivan, R. Guérin, M. Sergent, *Mater. Res. Bull*. **1988**, *23*, 891 – 898.

[19] T. B. Massalski, P. R. Subramanian, H. Okamoto, L. Kacprzak, *Binary Alloys Phase Diagrams*, Vol. 1 – 2, ASM International, Metals Park, Ohio, **1990**, p. 2223.

[20] K. H. J. Bushow, A. S. Van der Goot, *J. Less-Common Met*. **1970**, *22*, 419 – 428.

[21] V. Virkar, A. Raman, *J. Less-Common Met*. **1969**, *18*, 59 – 66.

[22] N. Ilnytska, L. G. Akselrud, S. I. Mykhalenko, Yu. B. Kuz'ma, *Kristallografiya* **1987**, *32*, 26 – 28.

[23] S. Oryshchyn, V. Babizhetskyy, S. Chykhrij, L. Akselrud, S. Stoyko, J. Bauer, R. Guérin, Yu. Kuz'ma, *Inorg. Mater*. **2004**, *40*, 450 – 456.

[24] R. L. Withers, J. G. Thompson, A. D. Rae, G. L. Hua, T. R. Welberry, A. C. Willis, R. Vincent, *Phase Transition*, New York, **1989**, *16/17*, pp. 47 – 51.

[25] L. G. Aksel'rud, Yu. N. Grin, V. K. Pecharsky, P. Yu. Zavalij, CSD97 (version No. 7), Universal Program Package for Single Crystal and Powder Data Treatment, **1997**.

[26] COLLECT, DENZO, Kappa CCD Program Package, Nonius BV, Delft (The Netherlands) **1998**.
[27] M. Zelinska, O. Zhak, S. Oryshchyn, J.-Y. Pivan, *Visnyk Lviv. Univ. Ser. Khim*. **2006**, *47*, 57 – 64.
[28] S. I. Chykhrij, V. S. Babizhetskyy, S. V. Oryshchyn, Yu. B. Kuz'ma, *J. Alloys Comp*. **1997**, *259*, 186 – 190.
[29] S. Chykhrij, V. Babizhetskyy, S. Oryshchyn, L. Aksel'rud, Yu. Kuz'ma, *Kristallografiya* **1993**, *38*, 262 – 265.
[30] J.-Y. Pivan, R. Guérin, *J. Less-Common Met*. **1986**, *120*, 247 – 254.
[31] W. Jeitschko, L. J. Terbüchte, U. Ch. Rodewald, *Z. Anorg. Allg. Chem*. **2001**, *627*, 2095 – 2099.
[32] R. Guérin, E. Chadraoui, J.-Y. Pivan, J. Padiou, M. Sergent, *Mater. Res. Bull*. **1984**, *19*, 1257 – 1270.
[33] J.-Y. Pivan, R. Guérin, *J. Solid State Chem*. **1998**, *135*, 218 – 227.
[34] S. Stoyko, S. Oryshchyn, V. Babizhetskyy, R. Guérin, *Z. Kristallogr. NCS* **2006**, *221*, 434 – 435.
[35] J.-Y. Pivan, R. Guérin, M. Sergent, *C. R. Acad. Sci. Paris, Ser. II*. **1984**, *299*, 689 – 692.
[36] J.-Y. Pivan, R. Guérin, M. Sergent, *Inorg. Chim. Acta*. **1985**, *109*, 221 – 224.
[37] S. I. Chykhrij, Yu. B. Kuz'ma, V. N. Davydov, S. L. Budnyk, S. V. Oryshchyn, *Kristallografiya* **1998**, *43*, 548 – 552.
[38] J.-Y. Pivan, R. Guérin, M. Sergent, *Mater. Res. Bull*. **1985**, *20*, 887 – 896.
[39] S. Chykhrij, L. Aksel'rud, S. Oryshchyn, Yu. Kuz'ma, *Dopov. Akad. Nauk. Ukr. RSR, Ser. B* **1985**, *11*, 58 – 61.
[40] J.-Y. Pivan, R. Guérin, J. Padiou, M. Sergent, *J. Less-Common Met*. **1986**, *118*, 191 – 200.
[41] S. Stoyko, S. Oryshchyn, V. Babizhetskyy, R. Guérin, *J. Alloys Comp*. **2004**, *367*, 156 – 161.
[42] S. I. Chykhrij, S. V. Oryshchyn, Yu. B. Kuz'ma, T. Glowiak, *Krystallografiya* **1989**, *34*, 1131 – 1135.
[43] M. Reehuis, T. Vomhof, W. Jeitschko, *J. Less-Common Met*. **1991**, *169*, 139 – 145.
[44] J.-Y. Pivan, R. Guérin, E. H. El Ghadraoui, M. Rafiq, *J. Less-Common Met*. **1989**, *153*, 285 – 292.
[45] E. H. El Ghadrahoui, J.-Y. Pivan, O. Pena, R. Guérin, P. Bonville, *Physica B*, **1990**, *163*, 185 – 187.
[46] V. Babizhetskyy, K. Hiebl, A. Simon, *J. Alloys Comp*. **2006**, *413*, 17 – 25.
[47] W. Jeitschko, L. J. Terbüchte, U. Ch. Rodewald, *Z. Anorg. Allg. Chem*. **2001**, *627*, 2673 – 2679.
[48] W. Jeitschko, L. J. Terbüchte, U. Ch. Rodewald, *Z. Naturforsch*. **2001**, *56b*, 1281 – 1288.
[49] N. Wiberg, *Holleman-Wiberg Lehrbuch der anorganischen Chemie*, de Gruyter, Berlin, **1995**, pp. 1838 – 1840.